Programmable computational RNA droplets assembled via kissing-loop interaction

Hirotake Udono,[1] Minzhi Fan,[1] Yoko Saito,[1] Hirohisa Ohno,[2,3] Shin-ichiro M. Nomura,[4] Yoshihiro Shimizu,[5] Hirohide Saito,[2,3] Masahiro Takinoue[1*]

1 Department of Computer Science, Institute of Technology, Midori-ku, Yokohama, Kanagawa, 226-8502, Japan

2 Graduate School of Medicine, Kyoto University, Sakyo-ku, Kyoto, 606-8501, Japan

3 Department of Life Science Frontiers, Center for iPS Cell Research and Application, Kyoto University, Sakyo-ku, Kyoto, 606-8507, Japan

4 Department of Robotics, Graduate School of Engineering, Tohoku University, Aoba-ku, Sendai, Miyagi, 980-8579, Japan

5 Laboratory for Cell-Free Protein Synthesis, Quantitative Biology Center, RIKEN, Suita, Osaka, 565-0874, Japan

*E-mail: takinoue@c.titech.ac.jp

This file includes:

- **Supporting notes, tables, and figures**

- **List of supporting movies**

Movie S1. Inputs of m1 and m2. Phase change from liquid to dispersed states.

Movie S2. Input of m1 only. No phase change.

Movie S3. Input of m2 only. No phase change. Pore formation due to increased structural flexibility.

Movie S4. Input of buffer. No phase change.

Movie S5. Inputs of m3 and m4. No phase change.

1. Sequences

Below are listed tables of the DNA/RNA sequences used in this study. Sticky ends (SEs) and kissing loops (KLs) are marked by bold fonts. In each motif, hybridized domains are colored in the same color, while the spacers ('TT' and 'UU') are in gray. We designed and verified the motifs with the help of NUPACK, a well-known software suite for design and analysis of nucleic-acid constructs.[1] The DNA sequences were purchased from Eurofins Genomics (Tokyo, Japan); The RNA sequences and miRNAs were from Sangon Biotech (Shanghai, China) and Hokkaido System Science Co. Ltd. (Sapporo, Japan). Upon arrival, they were dissolved into dH_20 and stored in a –30°C freezer until use.

1.1 X-motif with SEs

Table S1 X-motif DNA with SEs (dSE-X)[2]

Name	Sequence (5'–3')
dSE-X1	GCTCGAGCGCTGGACTAACGGAACGGTTAGTCAGGTATGCCAGCAC
dSE-X2	GCTCGAGCGTGCTGGCATACCTGACTTTCGCAAATTTACAGCGCCG
dSE-X3	GCTCGAGCCGGCGCTGTAAATTTGCGTTCATCACTTGGGACCATGG
dSE-X4	GCTCGAGCCCATGGTCCCAAGTGATGTTCCGTTCCGTTAGTCCAGC

Table S2 X-motif RNA with SEs (rSE-X)

Name	Sequence (5'–3')
rSE-X1	GCUCGAGCGCUGGACUAACGGAACGGUUAGUCAGGUAUGCCAGCAC
rSE-X2	GCUCGAGCGUGCUGGCAUACCUGACUUUCGCAAAUUUACAGCGCCG
rSE-X3	GCUCGAGCCGGCGCUGUAAAUUUGCGUUCAUCACUUGGGACCAUGG
rSE-X4	GCUCGAGCCCAUGGUCCCAAGUGAUGUUCCGUUCCGUUAGUCCAGC

1.2 X-motif with KLs

In addition to KL_Ori-X (Table S3), we designed two X-motif RNAs with weaker KL–KL interaction by adapting the self-complementary subsequence in the KL: We replaced two GC base-pairs (bps) with two AUs for KL_Mut1-X and with two GUs (wobble bps) for KL_Mut2-X. In the KL interaction, two KLs first form a helix via the Watson–Crick base-pairing in the self-complementary segments (underlined in the Tables), and then establish the tertiary structure via the coaxial stacking between the two loops.

Table S3 X-motif RNA with KLs (KL_Ori-X)

Name	Sequence (5′–3′)
KL_Ori-X1	**CUUGCUGAAGCGCGCACGGCAAG**GCUGGACUAACGGAACGGUUAGUCAGGUAUGCCAGCAC
KL_Ori-X2	**CUUGCUGAAGCGCGCACGGCAAG**GUGCUGGCAUACCUGACUUUCGCAAAUUUACAGCGCCG
KL_Ori-X3	**CUUGCUGAAGCGCGCACGGCAAG**CGGCGCUGUAAAUUUGCGUUCAUCACUUGGGACCAUGG
KL_Ori-X4	**CUUGCUGAAGCGCGCACGGCAAG**CCAUGGUCCCAAGUGAUGUUCCGUUCCGUUAGUCCAGC

Table S4 X-motif RNA with KLs (KL_Mut1-X)

Name	Sequence (5′–3′)
KL_Mut1-X1	…GAGCUC…
KL_Mut1-X2	…GAGCUC…
KL_Mut1-X3	…GAGCUC…
KL_Mut1-X4	…GAGCUC…

The omitted segments (…) are equal to the non-modified regions of the counterparts of KL_Ori-X.

Table S5 X-motif RNA with KLs (KL_Mut2-X)

Name	Sequence (5′–3′)
KL_Mut2-X1	…GGCGUU…
KL_Mut2-X2	…GGCGUU…
KL_Mut2-X3	…GGCGUU…
KL_Mut2-X4	…GGCGUU…

The omitted segments (…) are equal to the non-modified regions of the counterparts of KL_Ori-X.

1.3 Branched RNA motif capable of sensing targeted specific miRNAs

In the sensing RNA motif (Table S6), STH1,2 include a short single-stranded overhang as a toehold (underlined by dashed lines), which prefers to bind with the complementary region of the target miRNAs (m1 and m2, respectively. See Table S7) and initiate the strand displacement reaction. Only in the presence of m1 and m2, the 4-valence sensing RNA motif splits up into two 2-valence motifs. Otherwise, the valence is conserved, although the structural flexibility increases in the input of only m1 or m2. The displaced strand becomes a single-stranded extension protruding from the neighboring branch. The KL regions were adapted from those of KL_Mut2 (Table S5).

The set of miRNAs used herein (Table S7) is the tumor marker for detecting early-stage breast cancer.[3]

In the fluorescence recovery after photobleaching (FRAP) experiments described below, we labeled the sensing RNA motif by replacing 0.5 μM of KL_Mut2-Xs2 (10% of the final concentration) with 0.5 μM FAM-labeled ssDNA (Table S8) instead of adding the staining reagents.

Table S6 Sensing RNA motif with KLs (KL_Mut2-Xs)

Name	Sequence (5′–3′)
STH1	CACGACCGACGCCACUUCCGUUCCGUUAGUCCAGC
STH2	CCUGCUCCAAAAAUCUUCGCAAAUUUACAGCGCCG
KL_Mut2-Xs1	**CUUGCUGAAGGCGUUACGGCAAG**GCUGGACUAACGGAACGGUUAGUCAGGUAUGCCAGCAC
KL_Mut2-Xs2	**CUUGCUGAAGGCGUUACGGCAAG**GUGCUGGCAUACCUGACUUUGAUUUUUGG
KL_Mut2-Xs3	**CUUGCUGAAGGCGUUACGGCAAG**CGGCGCUGUAAAUUUGCGUUCAUCACUUGGGACCAUGG
KL_Mut2-Xs4	**CUUGCUGAAGGCGUUACGGCAAG**CCAUGGUCCCAAGUGAUGUUGUGGCGUCG

Table S7 miRNAs[3] (m1,2: target; m3,4: non-target)

Name	Sequence (5′–3′)
hsa-miR-1307-3p as ‘m1’	ACUCGGCGUGGCGUCGGUCGUG
hsa-miR-1204 as ‘m2’	AAUGGAUUUUUGGAGCAGG
hsa-miR-6875-5p as ‘m3’	UGAGGGACCCAGGACAGGAGA
hsa-miR-4634 as ‘m4’	CGGCGCGACCGGCCCGGGG

Table S8 FAM-labeled DNA sequence

Name	Sequence (5′–3′)
FAM_dXs2	[FAM]-GTGCTGGCATACCTGACTTTTTTGG

2. Native PAGE

The motifs listed above were analyzed by non-denaturing polyacrylamide gel electrophoresis (native PAGE). A mixture of 5.0 mL 40 w/v%-Acrylamide/Bis Partitioned Solution (29:1, Nakalai Tesque, Kyoto, Japan) and 4.0 mL 5× TBE (Tris-borate EDTA Buffer, Nippon Gene, Toyama, Japan) was topped up to 20 mL with dH_2O in a test tube to prepare an 8 cm × 8 cm gel plate with 10% concentration. After adding 150 µL of 10 w/v% APS (ammonium persulfate, FUJIFILM Wako Pure Chemical Corp.), the tube was gently inverted several times. After adding 3.0 µL TEMED (N, N, N’, N’- tetramethylethylenediamine, FUJIFILM Wako Pure Chemical Corp.), the tube was again inverted similarly. For polymerization, the solution was incubated for 60 min in an assembled gel electrophoresis cassette (BE-240G, Bio Craft, Tokyo, Japan).

Next, a 1.0 µL 1:1 mixture of a sample solution and a 2× loading buffer was loaded into each lane. 1.0 µL 10-bp ladder was loaded in the leftmost lane. The 2× loading buffer contained 1.0 w/v% BPB (bromophenol blue, FUJIFILM Wako Pure Chemical Corp.), 10 v/v% glycerol (FUJIFILM Wako Pure Chemical Corp.), and 500 mM EDTA (ethylenediaminetetraacetic acid, Nippon Gene). Afterward, gel electrophoresis was conducted at RT with a PowerPac Basic Power Supply (Bio-Rad Laboratories, CA, US) for 30 min at a constant voltage of 200 V in a cooler box (~4°C). The 10-bp ladder was a lab-fabricated mixture of purified polyT dsDNAs of 10–100 bp. The HPLC-purified polyTs were purchased from Eurofins. Finally, for fluorescence staining, the gel

plate was soaked and gently shaken at RT for 5 min in 100 mL 1× TBE containing 0.01 v/v% SYBR Gold. Finally, the gel plate was scanned by a 473-nm excitation laser and imaged by a fluorescence image analyzer (FLA-5100, Fujifilm, Tokyo, Japan).

The native PAGE showed that in each motif, the distinct bands for its component strands disappeared in the rightmost lane for the self-assembled condensates after 2 h incubation.

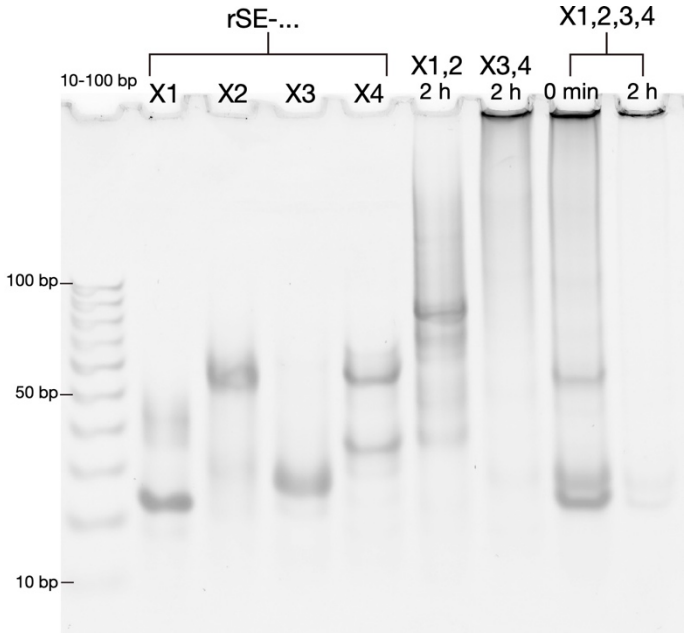

Figure S1 Native Page analysis of rSE-X. The time periods mean an incubation time length.

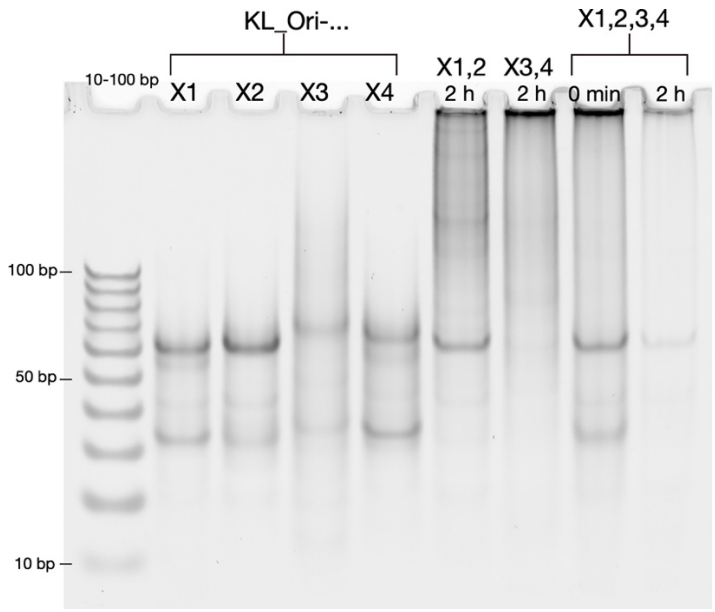

Figure S2 Native Page analysis of KL_Ori-X. The time periods mean an incubation time length.

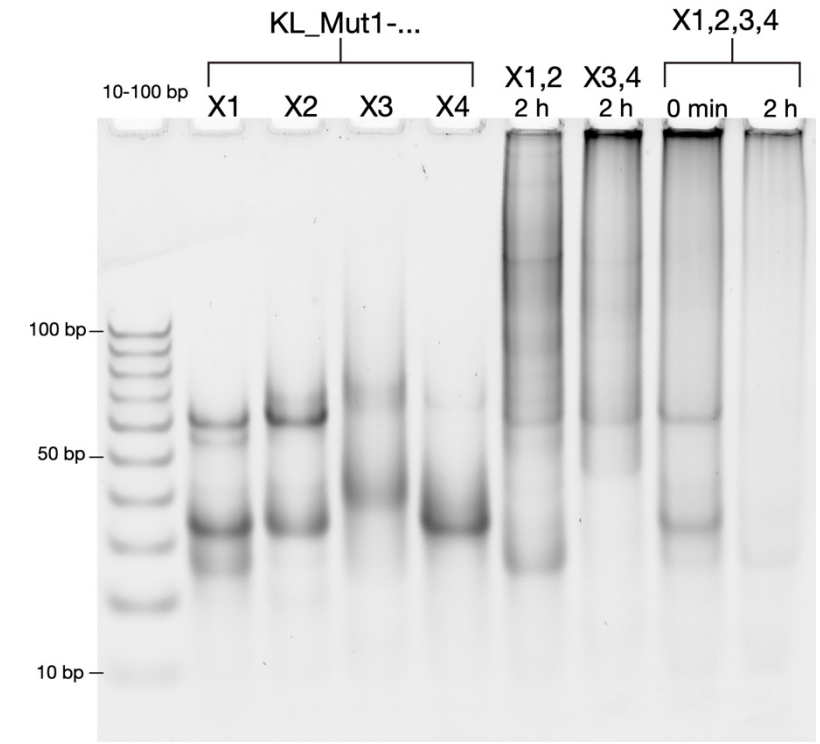

Figure S3 Native Page analysis of KL_Mut1-X. The time periods mean an incubation time length.

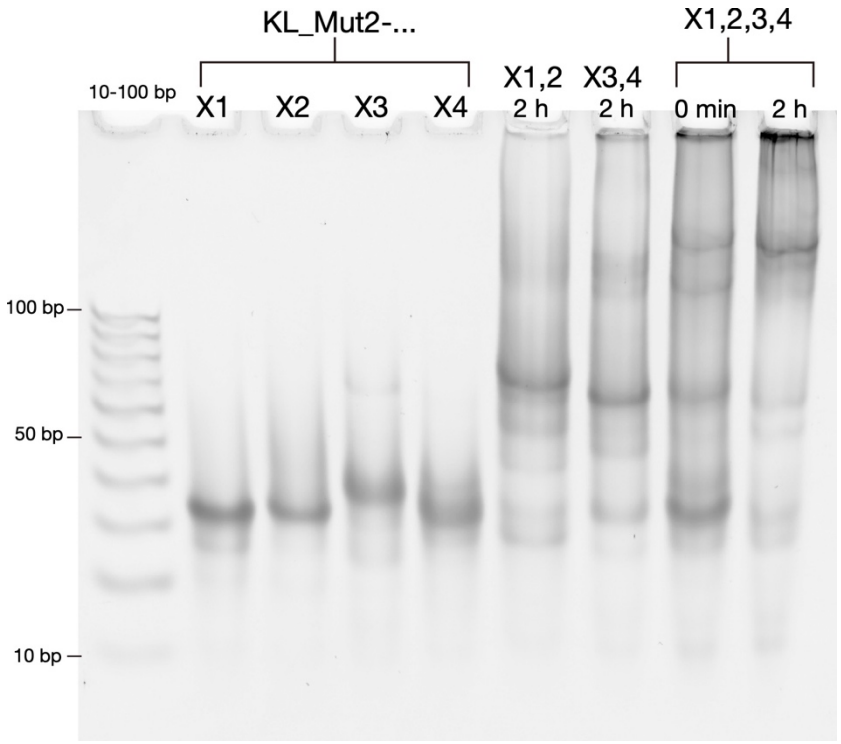

Figure S4 Native Page analysis of KL_Mut2_X. The time periods mean an incubation time length.

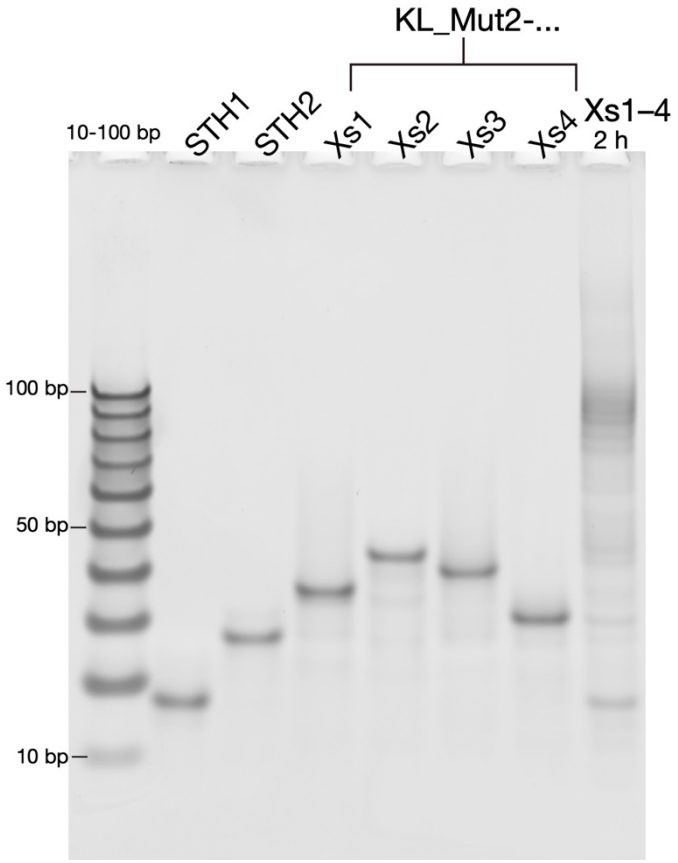

Figure S5 Native Page analysis of KL_Mut2_Xs. The time periods mean an incubation time length.

3. Construction of condensates

Throughout our experiments, we constructed condensates from the sequences listed above (Table S1–Table S6): An equimolar mixture of single-stranded sequences (ssDNAs or ssRNAs) was dissolved into an aqueous buffer within a PCR tube, with the final concentration of 5.0 μM for each ssDNA/RNA, 350 mM for NaCl (> 99.5% purity, FUJIFILM Wako Pure Chemical Corp.), and 20 mM for Tris-HCl pH8.0 (UltraPure, Thermo Fisher Scientific, MA, US). For confocal microscopy observation, the following fluorescent dyes were also added: 1000× Quant-iT^{TM} OliGreen (ssDNA Reagent, Thermo Fisher Scientific) for studying the SE–SE/KL–KL interaction strength (Figure 2) and 10000× SYBR^{TM} Gold (Nucleic Acid Gel Stain, Thermo Fisher Scientific) for demonstrating the AND logic operation (Figure 5). The mixed solutions were incubated at a fixed temperature of 25°C in a plate thermal cycler (Mastercycler® nexus flat, Eppendorf, Hamburg, Germany) for >2 h to allow for the self-assembly of nanostructures into the condensate of DNA or RNA.

4. Observation methods

For the fluorescence microscopy observation (Figures 2, 4, 5) and FRAP experiments (Figure 4), we used

a confocal laser scanning microscope (FV1000, Olympus, Tokyo, Japan). For the phase-contrast (PC) imaging (Figure 4b), the coalescence dynamics of RNA droplets were visualized using fluorescence microscopy (IX71, Olympus). The applied temperatures were regulated by a Peltier heating stage (10021-PE120, Linkam Scientific Instruments Ltd., Surrey, UK) in the confocal microscopy and a thermoplate (TPi-110RX, Tokai Hit Co., Ltd., Fujinomiya, Japan) in the PC imaging.

A sample solution was applied in a silicon sheet cavity as an observation chamber, where a punch-holed silicon rubber sheet of 1.0 mm in thickness (As One, Osaka, Japan) was affixed onto a 3.0 mm × 4.0 mm glass plate with a thickness of 0.13–0.17 mm (No.1, Matsunami Glass Ind., Ltd., Kishiwada, Japan). The glass plate was treated with a BSA (bovine serum albumin, FUJIFILM Wako Pure Chemical Corp.) solution of 5 w/v% BSA and 20 mM Tris-HCl in the experiments using the sensing RNA motif (Figure 4, 5).

5. Numerical evaluation of SE–SE/KL–KL interactions

For numerically evaluating the SE–SE binding strength (Figure 2), we used MELTING5,[4] free software for the prediction of melting temperatures of nucleic acids. In calculating the binding strength of dSE–dSE (Table S1) and rSE–rSE (Table S2), the components of the solutions as described above were entered in the input commands.

For numerically investigating the KL–KL interaction, we employed oxDNA,[5, 6] widely used coarse-grained numerical model for exploring the thermodynamic and structural properties of nucleic acids. The Monte Carlo simulations were performed on the following conditions: NVT ensemble at 30°C, 0.5 M sodium concentration, umbrella sampling with histograms being extrapolated to temperatures ranging from 25°C to 75°C, total time steps of 1.0×10^8, delta translation set as 0.15, and delta rotation as 0.2. Melting temperatures T_m (Figure 2) were obtained using a Python script from the generated histograms.

6. FRAP

In the FRAP experiments (Figure 4), the sensing RNA condensates self-assembled from KL_Mut2-Xs (Table S6) were photobleached to produce a bleached region of ~6 μm (19 pixels) on the surface as an ROI. The Peltier stage was set at 15°C and 30°C, at which the condensates would prefer a gel state and a liquid state, respectively. After capturing the time sequence over 30 min, the fluorescence recovery in the ROI was processed and analyzed using Fiji.[7] We noticed that in some cases, the RNA condensates experienced a disturbance-induced drift or slight fluorescence decay. To cancel out these effects on the quantification of the fluorescence recovery, we picked up a non-bleached region as a control in the data analysis process (Figure S6). We then calculated the ratio of the intensities from both regions, and rescaled it to a 0–1 range.

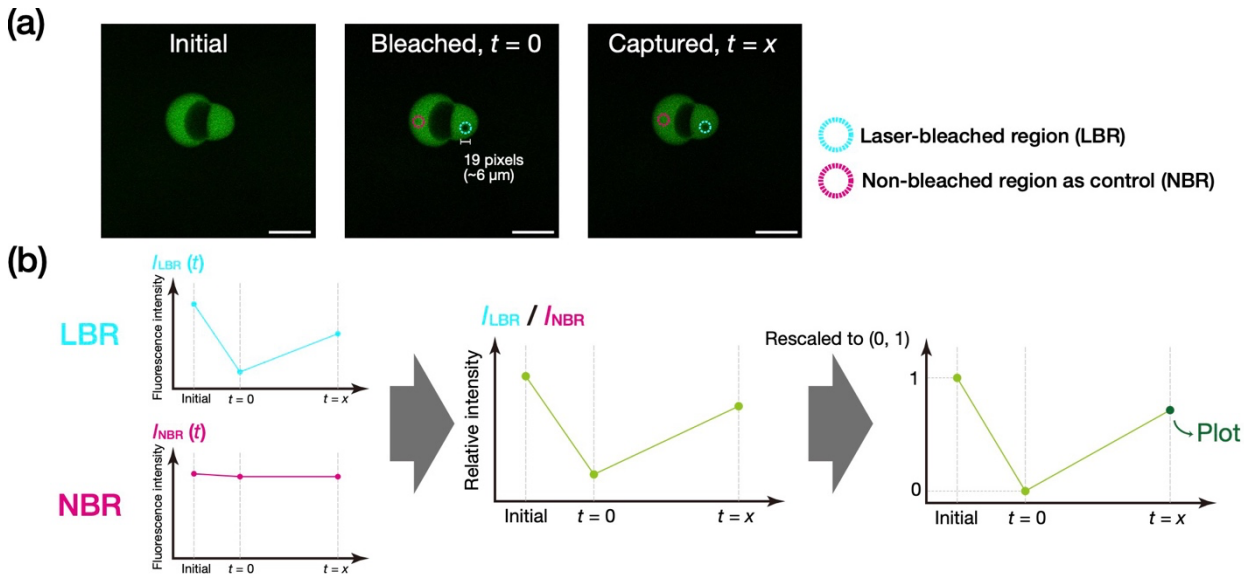

Figure S6 FRAP procedures. (a) Representative confocal microscopy images of photobleached RNA condensate (in a liquid-like state). Scale bars, 50 µm. (b) Description of the data analysis of captured fluorescence recovery.

7. AND logic operations

RNA condensate was assembled from KL_Mut2-Xs (Table S6) in a PCR tube at a fixed temperature of 25°C in the plate thermal cycler. Afterward, aqueous buffers containing miRNAs (Table S7) as an input were added, with a final concentration of [KL_Mut2-Xs] = 5.0 µM and [miRNA] = 5.0 µM. Following a two-hour incubation at 25°C, the sensing RNA condensate was visualized with FV1000 on the Peltier heating stage fixed at 30°C.

In the main manuscript, we demonstrated that inputs of both m1 and m2 created a drastic phase-state change in the RNA condensate from liquid to dispersed states, whereas an input of either m1 or m2 led to no significant phase change. To support this finding, we ascertained that the resulting phase states would not return to the initial state after a longer time period. In Figure S2, we observed the samples used in the input experiments after an overnight incubation at RT. In the inputs of m1 and m2, the dispersed state was conserved well; in the inputs of either m1 or m2, the dense phases were also preserved well, with a slight recovery in the fluorescence. This is firm evidence that the motif restructuring and resulting macroscopic conformations at 30°C suggested in Figure 5 was not a transient but a thermally irreversible process.

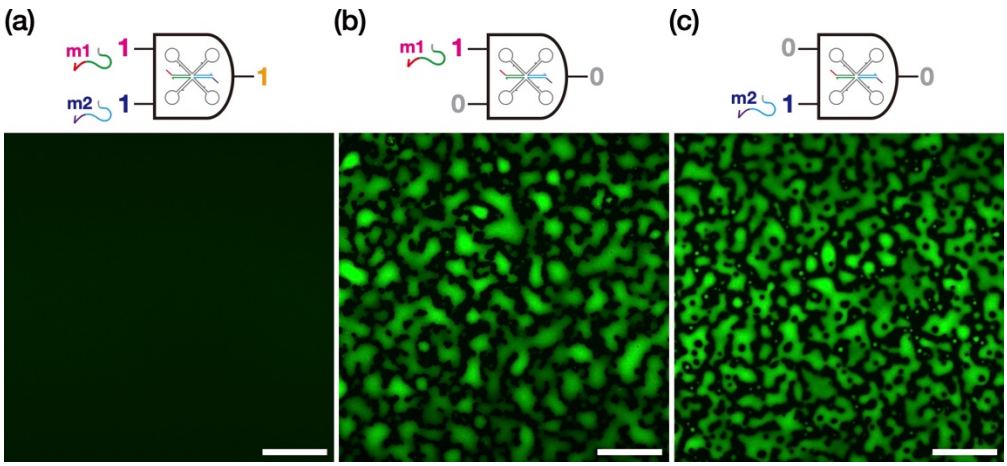

Figure S7 Thermal irreversibility of the computational process of RNA droplets. Confocal microscopy images of the samples observed one day after use in the input experiments. Inputs of (a) both m1 and m2, (b) only m1, and (c) only m2. Stainign dye, SYBR Gold. Scale bars, 50 µm.

SI REFERENCES

1. Zadeh JN, Steenberg CD, Bois JS, *et al.* NUPACK: Analysis and design of nucleic acid systems. *J Comput Chem*. 2011;32(1):170–173.
2. Sato Y, Sakamoto T, Takinoue M. Sequence-based engineering of dynamic functions of micrometer-sized DNA droplets. *Sci Adv*. 2020;6(23):eaba3471.
3. Shimomura A, Shiino S, Kawauchi J, *et al.* Novel combination of serum microRNA for detecting breast cancer in the early stage. *Cancer Sci*. 2016;107(3):326–334.
4. Dumousseau M, Rodriguez N, Juty N, Le Novère N. MELTING, a flexible platform to predict the melting temperatures of nucleic acids. *BMC Bioinformatics*. 2012;13:101.
5. Ouldridge TE, Louis AA, Doye JPK. Structural, mechanical, and thermodynamic properties of a coarse-grained DNA model. *J Chem Phys*. 2011;134(8):085101.
6. Snodin BEK, Randisi F, Mosayebi M, *et al.* Introducing improved structural properties and salt dependence into a coarse-grained model of DNA. *J Chem Phys*. 2015;142(23):234901.
7. Schindelin J, Arganda-Carreras I, Frise E, *et al.* Fiji: an open-source platform for biological-image analysis. *Nat Methods*. 2012;9(7):676–682.